JOURNAL OF VIROLOGY, Dec. 2003, p. 12852–12864 Vol. 77, No. 23
0022-538X/03/$08.00+0 DOI: 10.1128/JVI.77.23.12852–12864.2003
Copyright © 2003, American Society for Microbiology. All Rights Reserved.

Varicella-Zoster Virus-Infected Human Sensory Neurons Are Resistant to Apoptosis, yet Human Foreskin Fibroblasts Are Susceptible: Evidence for a Cell-Type-Specific Apoptotic Response

C. Hood,[1] A. L. Cunningham,[1] B. Slobedman,[1] R. A. Boadle,[2] and A. Abendroth[1]*

Centre for Virus Research, Westmead Millennium Institute and University of Sydney,[1] and Electron Microscope Laboratory, Westmead Millennium Institute and Institute of Clinical Pathology and Medical Research, Westmead Hospital,[2] New South Wales 2145, Australia

Received 19 May 2003/Accepted 20 August 2003

The induction of apoptosis or programmed cell death in virus-infected cells is an important antiviral defense mechanism of the host, and some herpesviruses have evolved strategies to modulate apoptosis in order to enhance their survival and spread. In this study, we examined the ability of varicella-zoster virus (VZV) to induce apoptosis in primary human dorsal root ganglion neurons and primary human foreskin fibroblasts (HFFs). Three independent methods (annexin V, TUNEL [terminal deoxynucleotidyltransferase-mediated dUTP-biotin nick end labeling] staining, and electron microscopy) were used to assess apoptosis in these cells on days 1, 2, and 4 postinoculation. By all three methods, apoptosis was readily detected in VZV-infected HFFs. In stark contrast, apoptosis was not detected during productive VZV infection of neurons. The low-passage clinical isolate Schenke and the tissue culture-adapted ROka strain both induced apoptosis in HFFs but not in neurons, suggesting that this cell-type-specific apoptotic phenotype was not VZV strain specific. These data show that the regulation of apoptosis differs markedly between HFFs and neurons during productive VZV infection. Inhibition of apoptosis during infection of neurons may play a significant role in the establishment, maintenance, and reactivation of latent infection by promoting survival of these postmitotic cells.

Varicella-zoster virus (VZV) is a ubiquitious, human herpesvirus that causes the predominantly childhood disease chicken pox (varicella) during primary infection of susceptible individuals. After resolution of primary infection by the host immune system, the virus can establish a life-long, latent infection. Like other members of the *Alphaherpesvirinae* subfamily, VZV establishes a latent infection in cells of the dorsal root ganglia (DRG) (29, 37). At some stage later in life, VZV may reactivate to cause shingles (herpes zoster), a painful unilateral vesicular rash confined along one or more sensory dermatomes (28). Herpes zoster can be complicated by postherpetic neuralgia (PHN), a severe, chronic pain that may persist for months to years after the initial appearance of the herpes zoster rash (24, 36).

Apoptosis or programmed cell death is an energy-dependent process of cell suicide that is characterized by several morphological features, including cell shrinkage, chromatin condensation, DNA fragmentation, membrane asymmetry, and plasma membrane blebbing (72, 73, 78). Apoptosis plays an important role in eliminating cells that may prove harmful to the host if they survive. Hence, a wide range of stimuli can induce apoptosis, such as virus infections, cell developmental stages, and cellular metabolic changes due to chemical or radiation damage (54, 61, 70).

Virus-encoded regulation of apoptosis has been postulated to play a major role in the pathogenesis of a variety of virus infections. Some viruses have evolved mechanisms to inhibit apoptosis, others induce it, and some appear to perform both functions (34, 54). Inhibition of apoptosis is likely to enhance survival and spread, thereby maximizing the production of virus progeny during lytic infection or facilitating a persistent infection (7, 34, 54, 61, 70). In this respect, certain cell types have been found to be resistant to apoptosis after infection with several human herpesviruses, including, human cytomegalovirus, Epstein-Barr virus (EBV), Kaposi's sarcoma herpesvirus, and herpes simplex virus type 1 and 2 (HSV-1 and HSV-2) (3, 8, 10, 22, 40, 42, 48, 50, 59, 63, 65, 80–82). These viruses have evolved a diverse range of strategies for disrupting apoptosis, and some have been shown to coordinate multiple mechanisms of interference (7, 34, 54, 70).

It has also been proposed that some viruses may actively induce apoptosis as a mechanism of efficient dissemination of progeny virus while evading host inflammatory responses (70). Several human viruses, including human immunodeficiency virus, human papillomavirus, hepatitis B and C viruses, and rubella virus, have been shown to promote apoptosis (6, 15, 23, 47, 57, 66, 67, 82). Examples of herpesviruses include HSV-1 (38, 56, 58) and bovine herpesvirus type 1 (BHV-1) (25, 30, 79), which both induce apoptosis in activated T cells, and HSV-1 and HSV-2, which are proapoptotic during infection of dendritic cells (L. Bosnjak, unpublished data; C. Jones, unpublished data). EBV has been shown to induce apoptosis in Raji cells (41). VZV has also been reported to induce apoptosis in semipermissive Vero cells (African green monkey kidney cells) (60). To date, however, the impact of VZV infection on apoptosis in permissive human cell types relevant to viral disease has yet to be examined in detail.

In the present study, we sought to determine whether VZV induces apoptosis in productively infected primary human sen-

* Corresponding author. Mailing address: Centre for Virus Research, Westmead Millennium Institute, P.O. Box 412, Westmead, 2145 NSW, Australia. Phone: 61-2-98459123. Fax: 61-2-98459100. E-mail: allison_abendroth@wmi.usyd.edu.au.

sory ganglionic neurons and primary human foreskin fibroblasts (HFFs). Three independent methods (annexin V, TUNEL staining, and transmission electron microscopy [TEM]) were used to demonstrate that productive VZV infection induced apoptosis in HFFs but not in human sensory neurons. Furthermore, a clinical isolate (strain Schenke) and a tissue culture-adapted virus (ROka), both induced apoptosis in HFFs but not in neurons, suggesting this cell-type-specific apoptotic phenotype was not VZV strain specific.

MATERIALS AND METHODS

Cells and viruses. HFFs were grown in tissue culture medium Dulbecco modified Eagle medium (DMEM) (Gibco, Melbourne, Australia) supplemented with 10% heat-inactivated fetal calf serum (FCS; CSL, Parkville, Australia). The VZV strains used in these studies were Schenke a low-passage clinical isolate and the recombinant strain ROka, which was generated by using cosmids derived from the varicella vaccine strain (13). Virus was propogated in HFFs and then stored in tissue culture medium with 10% dimethyl sulfoxide (Sigma). For cell-associated VZV infections, the degree of VZV infection of the inoculating fibroblasts was scored by using a scale from 0 to 4+, where 0 corresponds to no detectable infection and 4+ corresponds to 100% cytopathic effect. Inoculation of HFFs or neuronal cultures was done by using HFFs showing a 2 to 3+ cytopathic effect.

Preparation and culture of dissociated human sensory ganglionic neurons. Human sensory ganglionic neurons were isolated from human fetuses at 14 to 20 weeks of gestation. Human fetal tissue was obtained from therapeutic terminations after informed consent and approval of the research project by the Western Sydney Health Service and University of Sydney Ethics Committees. DRG were dissected from the spine and gently cleaned of surrounding connective tissue and epineurium. DRG were enzymatically digested in Hanks calcium- and magnesium-free (Gibco, Melbourne, Australia) containing 0.25% trypsin (CSL, Parkville, Australia) and 0.05% collagenase (Sigma) for 30 min at 37°C. During this incubation, DRG were gently triturated every 10 min and then centrifuged at 270 × *g* at 4°C for 5 min. The cell pellet was resuspended in 10 ml of modified Eagle medium (MEM) with 9% heat-inactivated FCS and incubated at room temperature for 2 min to allow large clumps to settle to the bottom of the tube. The 9-ml surface layer was transferred to a fresh tube and centrifuged as previously described. The cell pellet was resuspended in 400 μl of MEM with double D-valine modification (Sigma), and 10 μl of the cell suspension was seeded into sterile 24-well tissue culture plates that contained Matrigel (Integrated Sciences)-coated glass coverslips (Menzel-Glaser, Mainz, Germany). This yielded a range of 200 to 500 neurons per well, depending on the number of DRG harvested. The neuronal cells were incubated for 20 min at 37°C to allow the cells to adhere prior to the addition of 1 ml of MEM with a double D-valine modification supplemented with 5% (vol/vol) Monomed (CSL), 10 mM L-glutamine (Gibco), 5.12 g of D-glucose (Sigma)/liter, 40 ng of 7S-natural mouse nerve growth factor (Integrated Sciences)/ml, 2% heat-inactivated FCS, 10 μg of gentamicin (CSL)/ml, and 10 μg of vancomycin/ml (CSL). Neuronal cultures were incubated at 37°C with 5% CO_2 and monitored for the next 5 days for axonal growth. This treatment consistently yielded cultures with 80% of cells identified as neurons as determined by cell morphology, and on day 3 postplating extensive axonal networks between neurons were observed.

VZV infection of dissociated human neurons and HFFs. Neuronal cultures were inoculated with VZV by adding 10^4 VZV-infected HFFs per well of neurons or were mock infected by adding 10^4 uninfected HFFs. HFFs were inoculated with VZV by adding 10^4 VZV-infected HFFs to 5×10^4 uninfected HFFs. Mock-infected HFFs were set up by adding 10^4 uninfected HFFs to 5×10^4 uninfected HFFs.

Antibodies. Rabbit polyclonal antibodies specific for VZV open reading frames (ORFs) ORF4, ORF29, and ORF62 were kindly provided by P. R. Kinchington (University of Pittsburgh). VZV-immune (immunoglobulin G [IgG]-purified) polyclonal human serum that predominantly detects late VZV proteins (glycoproteins) and nonimmune serum was kindly provided by A. M. Arvin (Stanford University). Alexa Fluor 594-conjugated annexin V (annexin V-AF594) and fluorescein isothiocyanate (FITC)-conjugated goat anti-rabbit IgG were obtained from Molecular Probes (Eugene, Oreg.). Allophycocyanin-conjugated mouse anti-human IgG and FITC-conjugated annexin V (annexin V-FITC) were obtained from Pharmingen (Hamburg, Germany). FITC-conjugated goat anti-human IgG was obtained from Caltag Laboratories.

Annexin V staining and flow cytometry. Aliquots of 10^5 cells were washed three times in phosphate-buffered saline (PBS) and resuspended in 100 μl of binding buffer (10 mM HEPES-NaOH [pH 7.4], 140 mM NaCl, 2.5 mM $CaCl_2$; Pharmingen). Positive control cells were treated with 5% ethanol for 5 min at 37°C. A total of 5 μl of annexin V-FITC and 2 μl of propidium iodide (PI; Pharmingen) were added to the positive control cells and test cells, followed by incubation at room temperature in the dark for 15 min. To control for nonspecific binding, annexin V or PI alone was added to the test cells. Negative controls included cells resuspended in binding buffer only. Cells were immediately analyzed by using FACSCalibur and CellQuest software (Becton Dickson). Cells showing red fluorescence (PI^+) due to PI uptake were considered necrotic (i.e., cells had lost their membrane integrity). Only cells that were PI^- (cells with intact membrane integrity), which also stained with annexin V-FITC (annexin V^+/PI^-) were considered apoptotic.

Immunostaining for VZV antigens and flow cytometry. Aliquots of 10^5 were washed in PBS and resuspended in 100 μl of fluorescence-activated cell sorting (FACS) staining buffer (PBS with 1% FCS and 0.2% sodium azide). The primary antibodies, VZV-immune or nonimmune polyclonal IgG, were diluted 1:100. Secondary mouse anti-human IgG-allophycocyanin conjugated antibody was diluted at 1:20. As a negative control, cells were incubated with nonimmune IgG-purified polyclonal human serum (diluted 1:100) to control for nonspecific antibody binding. All antisera were diluted in FACS staining buffer, and reactions were performed in the dark at 4°C for 30 min. The cells were washed between each antibody step by adding 2 ml of FACS staining buffer, followed by centrifugation and aspiration of the supernatant. After the final wash, cells were resuspended in FACS staining buffer and cell suspensions were immediately analyzed by using FACSCalibur and CellQuest software. Positive and negative staining with specific antibodies was determined by the level of fluorescence, higher or lower, than levels determined by <97% of the 10,000 cells from the same starting population when incubated with isotype control fluorochrome-conjugated antibodies.

VZV antigen and annexin V detection by immunofluorescence staining and confocal microscopy. Cells grown on coverslips were immunostained for VZV antigens after fixation with 4% paraformaldehyde (ProSciTech) for 30 min at room temperature and permeabilized by incubating them with 0.1% Triton X-100 (Sigma) for 10 min at room temperature. Coverslips were washed in PBS and incubated with blocking buffer (10% normal goat serum in PBS) at 37°C for 30 min. Primary antibodies (ORF4, ORF29, ORF62, and VZV-immune or nonimmune IgG-purified polyclonal human serum) were added at a 1:100 dilution in blocking buffer and then incubated at 37°C for 30 min. Coverslips were washed three times in PBS, and the secondary antibodies were added for 30 min in the dark at 37°C. Secondary antibodies included FITC-conjugated goat anti-human IgG and FITC-conjugated goat anti-rabbit IgG, diluted in blocking buffer at 1:100 and 1:200, respectively. After three washes in PBS, coverslips were mounted onto glass slides with Slowfade Antifade mounting fluid (Molecular Probes) and then examined by using a Leica laser scanning confocal microscope. In all immunostaining experiments, isotype control antibodies were used with mock- and VZV-infected cells to control for nonspecific antibody binding.

Cells evaluated for annexin V were incubated with annexin V-binding buffer (10 mM HEPES [pH 7.4], 140 mM NaCl, 2.5 $CaCl_2$; Sigma) at room temperature for 10 min, and then 10 μl of annexin V-AF594 was added for 15 min in the dark at room temperature. Positive control cells were incubated at 37°C with 5% ethanol prior to incubation with annexin V-binding buffer. Cells were washed again in annexin V-binding buffer for 10 min and mounted with SlowFade Antifade containing a DAPI (4′,6′-diamidino-2-phenylindole) nuclear counterstain (Molecular Probes). Slides were analyzed by using a Leica laser scanning confocal microscope.

To determine the percentage of cells that were viral antigen or annexin V positive, a total of 500 neurons or 1000 HFFs were counted by randomly selecting fields of ~50 neurons or ~200 HFFs (magnification, ×40).

TUNEL staining. Neuronal cells and HFFs grown on coverslips were fixed in 10% phosphate-buffered formalin for 15 min at room temperature and washed twice in PBS. Cells were incubated with 2 μg of proteinase K (Gibco)/ml in PBS for 15 min at 37°C and then washed three times in PBS. A total of 50 μl of 3′OH DNA labeling mix (1× terminal deoxynucleotidyl transferase [TdT] reaction buffer composed of 0.5 M potassium cacodylate [pH 7.2], 10 mM $CaCl_2$, and 1 mM dithiothreitol [Gibco], 50 μM biotin-14-dCTP [Gibco-BRL], and 0.2 U of TdT [Gibco]) was added to each coverslip, followed by incubation at 37°C for 30 min. Positive control coverslips were treated with 3 U of DNase I (Gibco) in 0.1 M sodium acetate and 5 mM $MgCl_2$ (pH 5.0) for 30 min at 37°C prior to the addition of the 3′OH labeling mix. The negative control coverslips were incubated with a labeling mix containing no TdT. Cells were washed three times in PBS, followed by incubation with 5 μg of streptavidin-FITC (Gibco)/ml in 5%

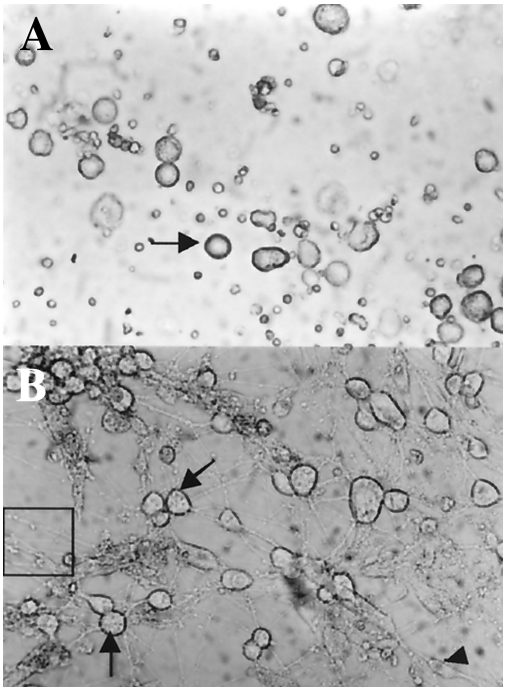

FIG. 1. Light microscopy of a typical dissociated human fetal DRG neuronal culture. (A) Neuronal culture immediately after dissociation containing spherical or tear-shaped neurons ranging from 10 to 50 μm (arrow). (B) Neuronal culture 3 days later containing neurons with extensive axonal networks (boxed area) and neurons congregating (arrows). Schwann cells and fibroblasts are planar and spindle-shaped (arrowheads).

skim milk in PBS for 30 min at 37°C. Coverslips were washed three times in PBS and mounted onto slides by using SlowFade Antifade mounting fluid with PI (Sigma) diluted 1:500 in PBS to determine cell viability. Cells were then analyzed by using a Leica laser scanning confocal microscope, and the percentage of TUNEL (TdT-mediated dUTP-biotin nick end labeling)-positive cells was calculated as described above.

TEM. Cells were fixed in modified Karnovsky's fixative for 1 h, washed twice in 0.1 M morpholinepropanesulfonic acid buffer (Sigma), postfixed in 2% buffered osmium tetraoxide for 3 h, followed by 2% aqueous uranyl acetate (Fluka, Switzerland) for 1 h, dehydrated through graded ethanols, and embedded in Spurr resin (TAAB Laboratories, Ltd.). Polymerization occurred at 70°C for 10 h. Ultrathin sections were cut by using a Reichert-Jung Ultracut E microtome, collected on 400-mesh thin-bar copper grids (TAAB), and stained with 1% uranyl acetate in 50% ethanol and Reynold's lead citrate. Sections were examined with a Philips CM120 BioTWIN transmission electron microscope at 80 kV.

RESULTS

Description of dissociated human dorsal root ganglia neuronal cultures. In order to assess the susceptibility of neurons to VZV-induced apoptosis, we first sought to establish primary human neuronal cultures. Human neuronal cells were cultured after enzymatic dissociation of human fetal DRG. Neuronal cultures consisted of predominantly sensory neurons and nonneuronal cells, including satellite cells, Schwann cells, and fibroblasts. On the day of plating neuronal cells, neurons ranged in size from 10 to 50 μm and appeared spherical with no axonal growth (Fig. 1A). After 3 to 5 days, ~80% of the culture consisted of sensory neurons with extensive axonal networks and nonneuronal cell types accounted for ~20% of the culture (Fig. 1B). As previously described, neurons were distinguished from nonneuronal cell types by their characteristic spherical or tear-shaped morphology, with sizes ranging from 10 to 50 μm in diameter and extensive uni- or bipolar axonal growth (51). In contrast, Schwann cells and fibroblasts have a flat and spindle-shaped morphology. These criteria were used throughout these studies to distinguish neurons from nonneuronal cells and to monitor the culture development. Neurons were defined as being suitable for subsequent VZV infection experiments based upon the appearance of extensive axonal networks.

Analysis of viral antigen expression in VZV-infected human sensory ganglionic neurons and fibroblasts. Using these human neuronal cultures, we assessed VZV infection and viral antigen expression in neurons compared to infection of HFF cultures. The full replicative cycle of VZV in permissive cells is presumed to follow a regulated cascade of viral gene expression (12). These viral genes can be defined into three temporal classes, immediate-early (IE), early (E), or late (L) gene products based upon their expression kinetics (43). Thus, we used a panel of antibodies to assess the expression and subcellular localization of representative viral genes from each kinetic class by immunofluorescence staining and confocal microscopy.

VZV is a highly cell-associated virus in experimentally infected cultures, and high-titer cell-free virus stocks cannot be generated (12, 76). Therefore, VZV-infected HFFs were used to inoculate human neuronal cultures. VZV strain Schenke-infected HFFs or uninfected HFFs (mock infection) were added to neuronal cells at a density of 10^4 HFFs/500 neurons. In parallel, HFFs were also infected with VZV strain Schenke by mixing 5×10^4 uninfected HFFs with 10^4 VZV-infected HFFs. On days 1, 2, and 4 postinfection (p.i.), mock- and VZV-infected neuronal cells and HFFs were subjected to immunofluorescence analysis for the immediate-early gene products ORF62 and ORF4, the early gene product ORF29, or late VZV proteins (glycoproteins). Negative controls included neuronal cells and HFFs incubated with uninfected HFFs (mock infected) and incubation of mock- and VZV-infected cells with isotype control antibodies to control for nonspecific binding of primary antibodies.

In VZV-infected neuronal cultures, VZV antigen-positive neurons were readily detectable at all time points tested (Fig. 2). The VZV immediate-early protein ORF62 was localized to the nucleus and cytoplasm of neurons (Fig. 2A). The early gene products ORF4 and ORF29 were localized to the cytoplasm and subcompartmental cytoplasmic vacuoles (Fig. 2B and 2C), respectively. Late viral antigens (glycoproteins) were localized predominantly to the cell surface of neurons (Fig. 2D). Viral antigens were also detected in small numbers of VZV-infected fibroblasts (used in the cell-associated inoculum) and Schwann cells (data not shown). Mock-infected neurons did not stain with any of the VZV antigen-specific antibodies (Fig. 2E). Isotype control antibodies did not stain either mock (data not shown)- or VZV (Fig. 2F)-infected cells. The subcellular localization of these viral gene products in neurons was consistent with that observed in VZV-infected HFFs with the exception of ORF29, which was localized to the nucleus of VZV-infected HFFs (data not shown).

To determine the proportion of neurons and HFFs infected with VZV a total of 500 neurons and 1,000 HFFs were counted

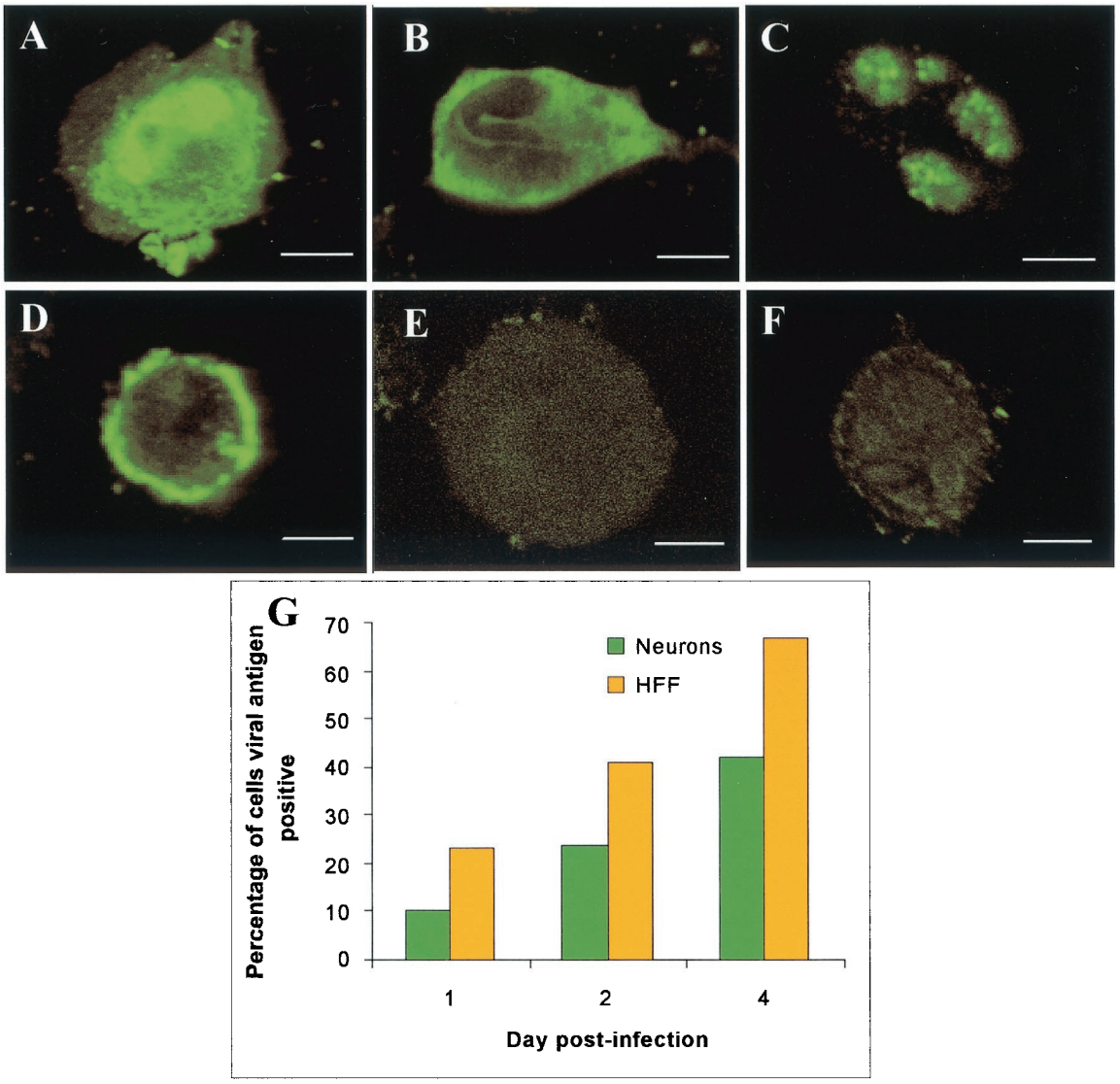

FIG. 2. Immunofluorescence analysis of viral antigen expression in VZV-infected neurons. At 2 days p.i., neurons infected with VZV strain Schenke (A to D and F) and mock infected (E) were incubated with rabbit polyclonal antibodies to ORF62 (A and F), ORF4 (B), ORF29 (C), and a hyperimmune serum that predominantly detects glycoproteins (D). Rabbit and human anti-VZV antibodies were detected by using FITC-conjugated secondary antibodies (green fluorescence). Negative controls were mock-infected neurons (E) or VZV-infected neurons incubated with an isotype control antibody (F). Negative control images were obtained by increasing the laser voltage to enable the visualization of cells. Bar, 10 μm. (G) Percentages of cells stained with the VZV hyperimmune polyclonal serum (VZV antigen-positive cells) for VZV-infected neuronal and HFF cultures over the 4-day time period.

after immunostaining with the VZV immune polyclonal serum at each time point (Fig. 2G). Neurons were clearly distinguished from inoculating VZV-infected HFFs on the basis of their spherical or tear-shaped morphology, sizes ranging from 10 to 50 μm in diameter, and extensive uni- and bipolar axonal growth. In neuronal cultures, there was a significant increase in the number of infected neurons detected over the time points tested, and the rate of increase of viral-antigen-positive neurons was comparable to that seen in HFFs. In repeated experiments with dissociated human neuronal cells from three different donors, VZV antigens from the three kinetic classes were readily detectable, and a similiar rate of increase in viral antigen positive neurons was observed over the 4-day time period. Due to the presence of VZV-infected HFFs in the culture from the cell-associated method of infection, it was not possible to perform an infectious center assay to directly determine whether new infectious virus particles were generated in VZV-infected neurons. As an alternative, we utilized TEM to demonstrate that numerous enveloped virions on the surfaces of neuronal cell bodies and unenveloped virions in the nucleus were present in VZV inoculated neuronal cultures (Fig. 8). Taken together, these data demonstrate that VZV could (i) infect, (ii) synthesize IE, E, and L viral proteins, and (iii) assemble virions in primary sensory neurons and HFFs and that the kinetics of productive infection was comparable between these two cell types.

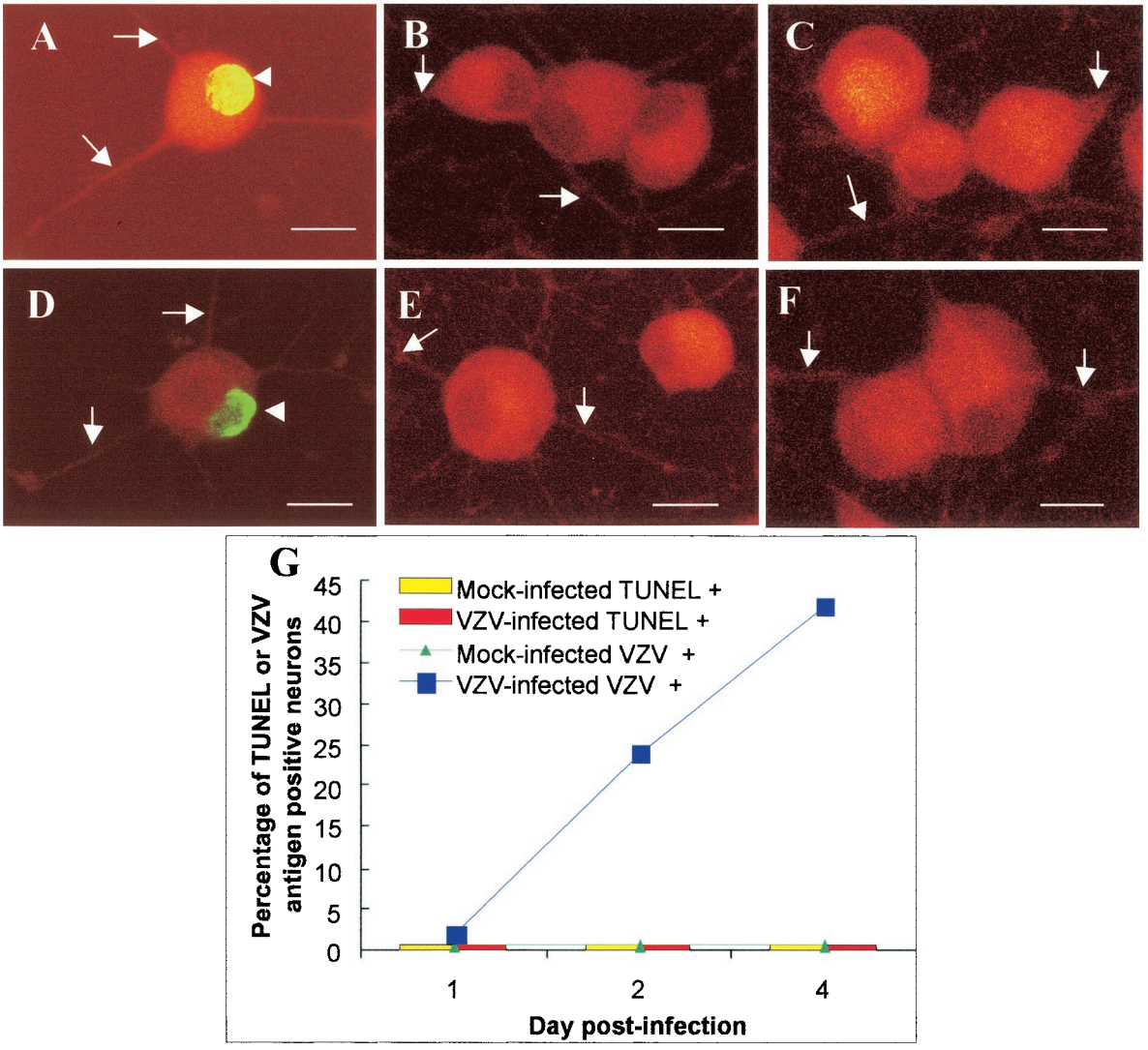

FIG. 3. Visualization and quantitation of apoptotic cells by the TUNEL assay in VZV-infected neuronal cultures. Neurons inoculated with VZV-infected HFFs (A to C) or uninfected HFFs (D to F) were harvested on day 2 postinoculation and processed for the TUNEL assay. No TUNEL-specific staining was detected in VZV-infected (B) or mock-infected (E) neuronal cultures. Positive controls were treated with DNase prior to labeling (A and D), and negative controls were treated with TdT reaction mix containing no TdT (C and F). Bars, 10 μm. Each arrow indicates the neuronal axons, and each arrowhead indicates the apoptotic nuclei (green fluorescence). (G) Percentages of neurons labeled for apoptotic nuclei ($TUNEL^+$) or VZV antigens (VZV^+) over the 4-day time course in mock- and VZV-infected neuronal cultures.

Assessment of DNA fragmentation in VZV-infected human neurons and fibroblasts. Cleavage of DNA into nucleosomal fragments is a characteristic marker of apoptosis (73, 78). To investigate the impact of VZV infection on the induction of apoptosis in neurons and fibroblasts, VZV-infected human neuronal cultures and HFFs were processed for the TUNEL assay, which detects fragmented DNA 3′OH termini (27).

Neuronal cultures and HFFs were mock or VZV infected as described above. On days 1, 2, and 4 p.i., coverslips containing neuronal cells or fibroblasts were processed for the TUNEL assay. Positive controls were mock- and VZV-infected neuronal cells and HFFs incubated with DNase prior to TdT labeling. Negative controls included mock- and VZV-infected cells incubated with 3′OH DNA labeling mixture containing no TdT. In parallel, duplicate coverslips were also processed for immunofluorescence staining and confocal microscopy to assess VZV antigen expression as described above. At each time point tested, 500 neurons or 1,000 HFFs per coverslip were counted for either fragmented DNA termini (TUNEL staining) or VZV antigen expression.

In VZV-infected or mock-infected neuronal cultures, neurons showed no staining for fragmented DNA termini at any of the time points tested (Fig. 3B and 3E). However, a proportion of VZV-infected HFFs (24%), which were present due to the cell-associated method of VZV infection, were staining for fragmented DNA termini at day 1 p.i. (data not shown). In contrast, the positive control DNase-treated, VZV- and mock-infected neuronal cultures showed 96 and 97% of neurons labeled for apoptotic nuclei, respectively (Fig. 3A and 3D). No staining of apoptotic nuclei were detected in VZV- or mock-

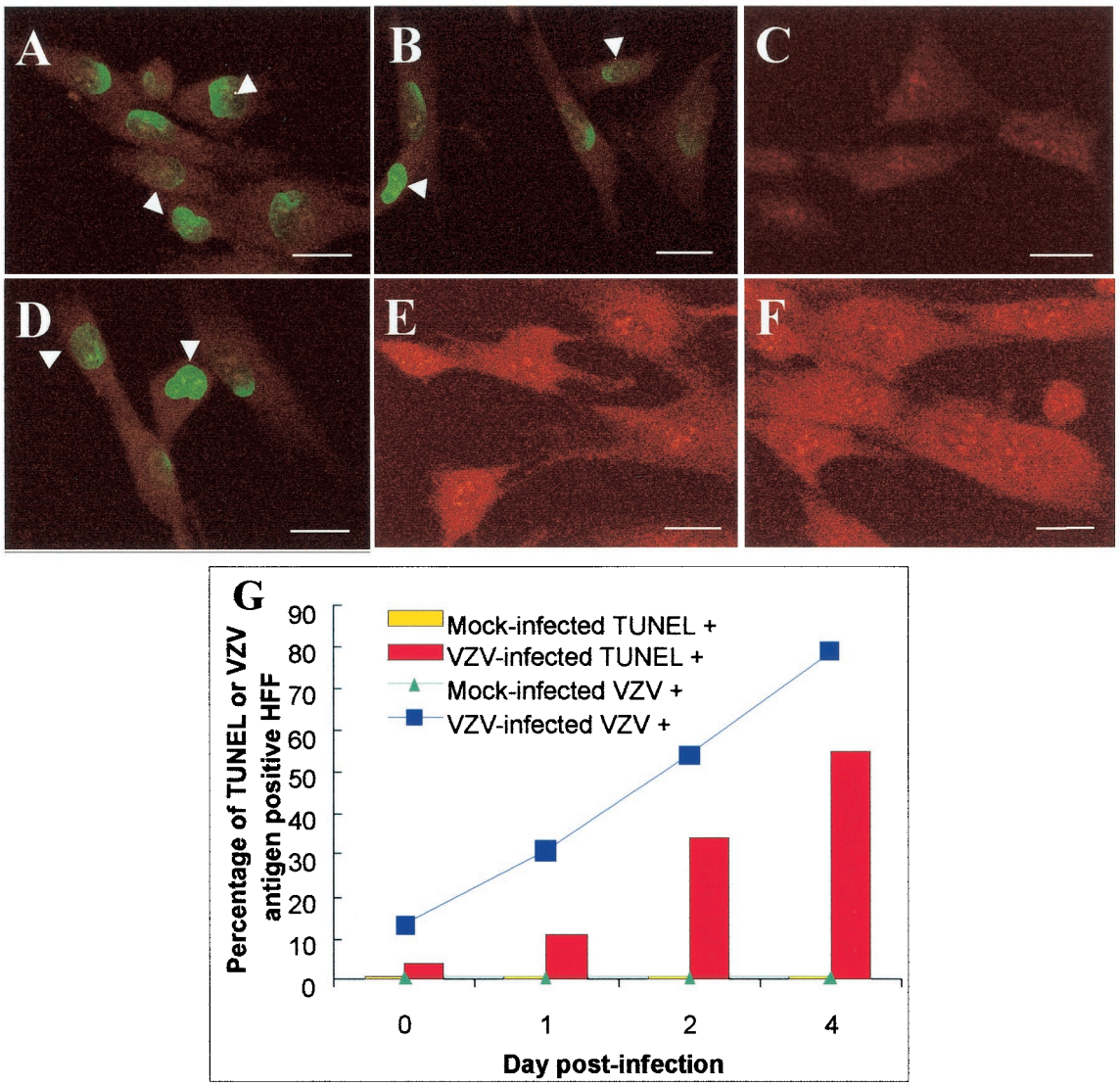

FIG. 4. Visualization and quantitation of apoptotic cells by the TUNEL assay in VZV-infected HFFs. VZV-infected HFFs (A to C) or uninfected HFFs (D to F) were harvested on day 2 postinoculation and processed for the TUNEL assay. (B) TUNEL-specific staining was detected in VZV-infected HFFs. (E) No TUNEL staining was detected in mock-infected HFFs. Positive controls were treated with DNase prior to labeling (A and D), and negative controls were treated with TdT reaction mix containing no TdT (C and F). Bars, 10 μm. Each arrowhead indicates the apoptotic nuclei (green fluorescence). (G) Percentages of HFFs labeled for apoptotic nuclei ($TUNEL^+$) or VZV antigens (VZV^+) over the 4-day time course in mock- and VZV-infected HFF cultures.

infected neuronal cultures incubated with 3′OH DNA labeling mix containing no TdT (Fig. 3C, 3F). Despite the detection of significant numbers of VZV antigen positive neurons at days 2 and 4 p.i., no TUNEL-positive neurons were detected (Fig. 3G). In a total of four replicate experiments with four different donors to generate human neuronal cultures, 40% ± 0.9% (mean ± the standard error of the mean) of the neurons expressed VZV antigens on day 4 p.i., with no neurons staining for fragmented DNA termini.

In contrast to VZV-infected neuronal cultures, between 4 and 55% VZV-infected HFFs stained for fragmented DNA termini over the 4-day time course (Fig. 4B). The positive control DNase-treated, VZV- and mock-infected HFFs showed 88 and 84% of HFFs labeled for apoptotic nuclei, respectively (Fig. 4A and 4D). No TUNEL staining was observed in mock-infected HFFs (Fig. 4E) or in VZV- or mock-infected HFFs incubated with 3′OH DNA labeling mix containing no TdT (Fig. 4C and 4F). In addition, the rate of increase of detectable TUNEL-stained cells and VZV antigen-positive HFFs was similar across the time course of infection (Fig. 4G). In a total of four replicate experiments, 66.8% ± 0.7% of HFFs expressed VZV antigens on day 4 p.i., with 45.6% ± 0.5% HFFs staining for fragmented DNA termini. Taken together, these data demonstrate that VZV infection induces detectable fragmentation in HFFs but not in human sensory neurons. This was despite neurons being exposed to a higher virus input. Thus, neurons appear to be protected against apoptosis after VZV infection.

Analysis of PS translocation in VZV-infected human neurons and fibroblasts. DNA fragmentation is a well-characterized late marker of apoptosis. An earlier marker of apoptosis is the exposure of phosphatidylserine (PS) from the inner to the outer leaflet of the cell membrane (26). Therefore, we assessed the effect of VZV infection of neurons and HFFs on PS translocation by utilizing annexin V, a protein that binds with high affinity to cell-surface exposed PS in the presence of calcium. On days 1, 2, and 4 p.i., coverslips containing mock- or VZV-infected cells were processed for either viral antigen staining as described above or annexin V staining. Positive controls included mock and VZV-infected cells incubated with 5% ethanol for 30 min at 37°C prior to staining. The percentage of neurons that were viral antigen or annexin V positive was determined by counting a total of 500 cells per time point.

When VZV-infected and mock-infected neuronal cultures were assayed for annexin V staining, <5% of the neurons were annexin V positive at any of the time points tested (Fig. 5E). However, as observed in the TUNEL staining analyses, a proportion of VZV-infected human fibroblasts (38%) (present due to the cell-associated method of VZV infection) were staining for annexin V (data not shown). The neuronal cultures treated with 5% ethanol showed 48 and 45% of neurons staining for annexin V in the VZV-infected and mock-infected cultures, respectively (Fig. 5A and C). No specific staining for annexin V was observed in VZV- or mock-infected neuronal cultures (Fig. 5B and D). In three replicate experiments with neuronal cultures derived from three different donors, 42% ± 0.5% of neurons expressed VZV antigens on day 4 p.i., with only 3.3% ± 0.2% neurons staining for annexin V, whereas in mock-infected cultures no neurons stained for VZV antigen and 4% ± 0.3% of neurons stained for annexin V.

In contrast, annexin V-positive HFFs were readily detected at the same time points when infected with VZV (Fig. 6B). The positive control (5% ethanol-treated) HFFs showed 44% ± 0.67% staining for annexin V in VZV-infected (Fig. 6A) and 33% ± 0.62% in mock-infected (Fig. 6C) HFFs. No specific annexin V staining was detected in mock-infected HFF (Fig. 6D). The percentage of annexin V-stained HFFs increased over the time course concomitant with an increase in the percentage of viral-antigen-positive cells (Fig. 6E). On average (from three independent experiments) by day 4 p.i., 52% ± 0.67% of VZV-infected HFFs staining for annexin V compared to only 8% ± 0.4% of mock-infected HFFs. These results demonstrate that VZV infection induces characterisitic apoptotic membrane changes such as PS exposure in HFFs but not in neurons.

Assessment of apoptosis in human neurons and fibroblasts infected with the ROka vaccine strain. To determine whether other VZV strains induced apoptosis in a cell-type-specific manner, we extended our studies to assess apoptosis in neurons and HFFs infected with a tissue culture-adapted recombinant Oka vaccine strain (ROka).

Human neuronal cultures and HFFs were inoculated with either VZV strain Schenke or ROka-infected HFFs or uninfected HFFs (mock infected) as detailed above. On days 1, 2, and 4 p.i., coverslips containing neuronal cells or fibroblasts were processed for the TUNEL assay, annexin V staining, and viral antigen staining (Fig. 7). The TUNEL and annexin V staining results demonstrated that both viruses induced comparable levels of apoptosis in HFFs, whereas neither virus induced apoptosis in neurons. Similar results were obtained in two replicate experiments. These data indicate that cell-type-specific regulation of apoptosis is a feature common to diverse VZV strains.

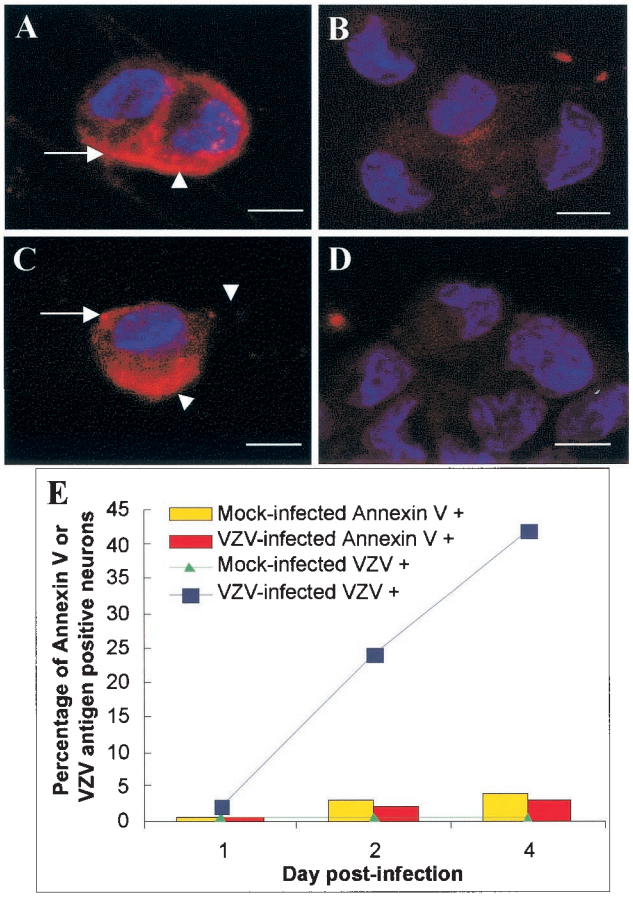

FIG. 5. Immunofluorescence analysis of membrane PS exposure associated with apoptosis by annexin V staining in VZV-infected neuronal cultures. At 2 days p.i., neurons inoculated with VZV-infected HFFs (A and B) or mock-infected HFFs (C and D) were incubated with annexin V-Alexa Fluor 594 conjugate (red fluorescence) and a nuclear counterstain DAPI (blue fluorescence) and then analyzed by laser confocal microscopy. Positive controls were VZV-infected (A) and mock-infected (C) cells treated with 5% ethanol prior to staining. No specific annexin V staining was detected in VZV-infected (B) or mock-infected (D) neuronal cultures. Bar, 10 μm. Neuronal axon hillocks are indicated by arrows, and arrowheads indicate annexin V staining. (E) Percentages of neurons staining for annexin V (annexin V^+) or VZV antigens (VZV^+) over the 4-day time course in mock- and VZV-infected neuronal cultures.

Analysis of cellular morphology in VZV-infected human neurons and fibroblasts by TEM. To further confirm VZV-mediated induction of apoptosis in HFFs but not neurons, TEM was used to assess specific ultrastructural changes in cellular morphology, which are indicators of apoptosis. On day 2 p.i. VZV-infected neurons and HFFs were fixed, harvested, and processed for TEM.

Human neurons were readily identifiable by their characteristic neuronal morphology and axonal processes. VZV-infected neurons appeared normal, possessing an intact double

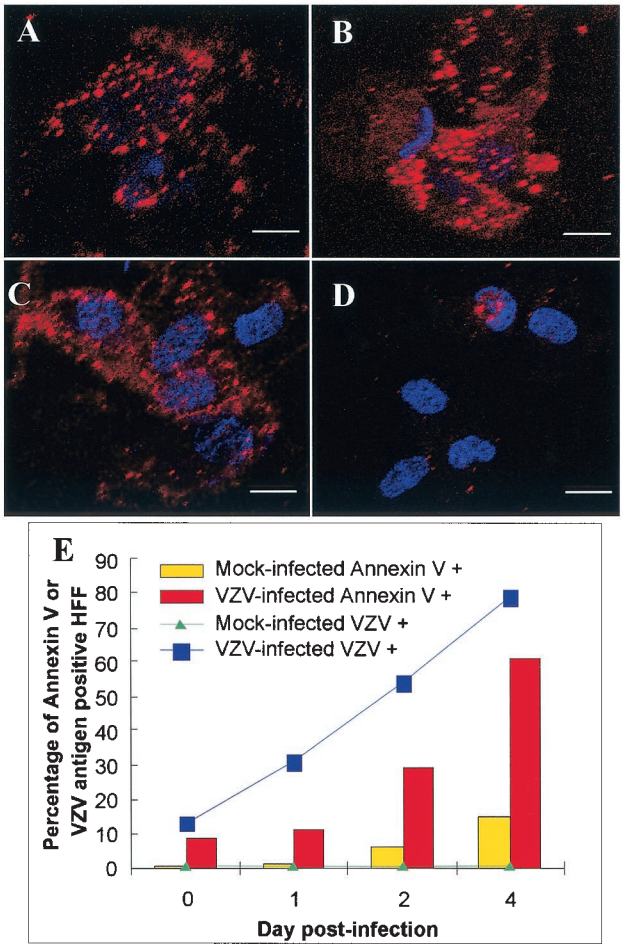

FIG. 6. Immunofluorescence analysis of membrane PS exposure associated with apoptosis by annexin V staining in VZV-infected HFFs. Two days p.i. VZV-infected HFFs (A and B) or mock-infected HFFs (C and D) were incubated with annexin V-Alexa Fluor 594-conjugate (red fluorescence) and a nuclear counterstain DAPI (blue fluorescence) and then analyzed by laser confocal microscopy. Positive controls were VZV-infected (A) and mock-infected (C) cells treated with 5% ethanol prior to staining. (B) Specific annexin V staining was detected in VZV-infected HFFs. (D) No staining was detected in mock-infected HFFs. Bar, 10 μm. An arrowhead indicates annexin V staining. (E) Percentages of neurons staining for annexin V (annexin V^+) or VZV antigens (VZV^+) over the 4-day time course in mock- and VZV-infected HFF cultures.

nuclear membrane with normal chromatin distribution and organelles, specifically Golgi apparatus, mitochondria, and endoplasmic reticulum (Fig. 8A). There are numerous unenveloped virions in the nucleus and enveloped virions on the surface of the cell body (Fig. 8A). In contrast, VZV-infected HFFs displayed characteristic ultrastructural features of apoptosis, including loss of the double nuclear membrane, condensation of chromatin, irregular organelle morphology, and an increased number of lipid vesicles (Fig. 8B). Enveloped virions appeared in the cytoplasm and on the cell surface (Fig. 8B). Examination of multiple VZV-infected neurons and HFFs revealed a similar intracellular localization and abundance of viral particles in these two different cell types, but ultrastructural changes in cellular morphology indicative of apoptosis were only observed in VZV-infected HFFs. Ultrastructural changes in cellular morphology indicative of apoptosis were not observed in mock-infected neurons or HFFs (data not shown). These results demonstrate that morphological changes associated with apoptosis were observed in VZV-infected HFFs but not in VZV-infected human neurons, despite the similar abundances of unenveloped and enveloped VZV virions within both cell types.

DISCUSSION

This study provides the first evidence of a cell-type-specific apoptotic response to VZV infection. We demonstrate here that VZV infection of HFFs induces changes indicative of apoptosis, including (i) DNA fragmentation (as seen by TUNEL staining), (ii) chromatin condensation, membrane blebbing, and irregular organelle morphology (as seen by TEM), and (iii) PS externalization at the cell membrane (as seen by annexin V staining). In stark contrast, apoptosis was not observed during VZV infection of human primary sensory neurons with any of the above methods.

Like all herpesviruses, a key feature in the life cycle of VZV is an ability to establish a life-long latent infection in the host from which it can reactivate years later, resulting in virus transmission to susceptible individuals. During primary infection, VZV accesses sensory neurons located within spinal ganglia, where it has the ability to initiate a productive infection, as demonstrated by the presence of productive viral transcripts and proteins (9, 16, 68, 69, 77). However, at some point after this infection, the virus establishes latency in these cells. The ability of VZV to successfully establish a latent infection in sensory neurons is dependent on the neuron remaining viable during this process. Thus, from the perspective of the virus, neuronal cell death during the establishment phase would be a clinically unfavorable outcome since it would decrease the possibility for future virus transmission in the human population. Indeed, during varicella there is no histological or clinical evidence of sensory neuropathy. It has previously been suggested that resistance to neuronal cell loss may be a result of these cells not supporting the complete lytic replicative cycle (62). Our finding of an antiapoptotic function during productive VZV infection of neurons provides evidence for an additional mechanism by which the virus would ensure the survival of the neuron, thus increasing its ability to efficiently establish a latent infection in these cells. The continued development of models to study the establishment of latency in neuronal cells will ultimately help to define the molecular mechanisms involved in this process.

In addition to a potential role during the establishment of latency, a neuron-specific antiapoptotic function may also be important during virus reactivation. Protecting neurons against apoptosis during the critical first stages of virus reactivation would allow for greater production of new virions for axonal transport to the skin and zoster lesion formation. In contrast to varicella, histological studies of DRG from postmortem cases of patients suffering from herpes zoster and postherpetic neuralgia have demonstrated extensive neuronal necrosis, cell body, axon and myelin loss, fibrosis, and intense inflammation (20, 35, 74). It has been postulated that the underlying cause of the pain (postherpetic neuralgia) associated with herpes zoster

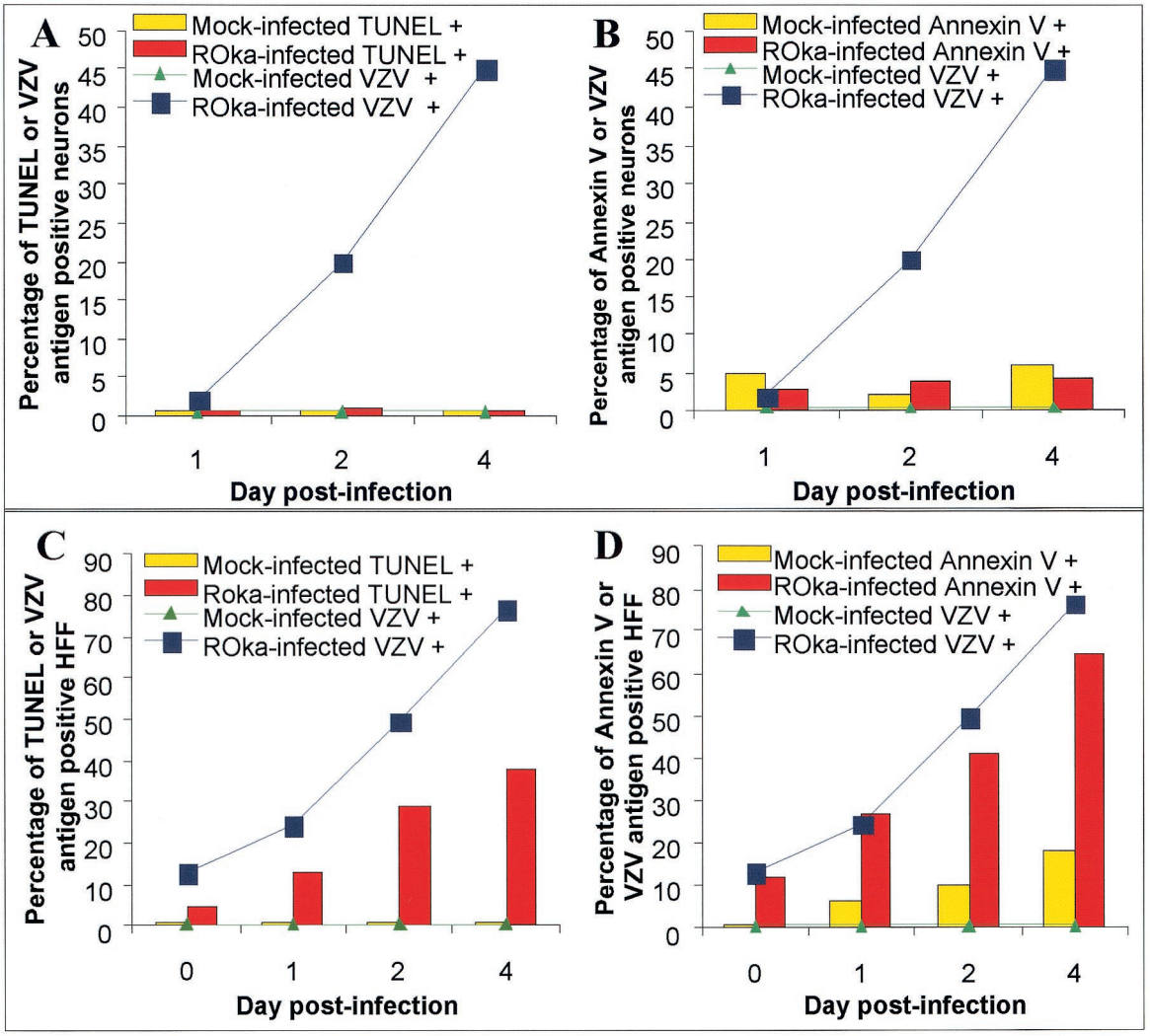

FIG. 7. Quantitation of apoptotic cells by the TUNEL assay and annexin V staining in VZV ROka-infected neuronal and HFF cultures. The percentages of neurons and HFFs staining for TUNEL (TUNEL$^+$), annexin V (annexin V$^+$), or VZV antigens (VZV$^+$) over the 4-day time course in mock and VZV-infected neuronal cultures (A and B) and mock- and VZV-infected HFF cultures (C and D) are shown.

is the damage to neural tissue caused by VZV reactivation (75). Our data suggest that this neuronal destruction may not be a result of virus-induced apoptosis. Rather, it may be a consequence of the host cellular immune response, an area of research that merits further investigation.

The identity of the VZV gene(s) encoding any antiapoptotic function in productively infected neurons remains to be elucidated. However, it is tempting to speculate as to potential VZV gene candidates given the previous identification of HSV gene products that effectively block apoptosis and the sequence similarities between these two alphaherpesviruses. In this respect, VZV ORF66 (64) is homologous to the HSV-1 and HSV-2 antiapoptotic gene product US3 (33, 46, 52). VZV ORF4, ORF62, and ORF63 share homology to the antiapoptotic HSV-1 genes ICP27, ICP4, and ICP22, respectively (4, 5, 45). These three VZV ORFs are expressed not only during productive infection but have also been detected in the cytoplasms of latently infected human neurons (14, 18, 49). The

FIG. 8. TEM images of VZV-infected human DRG neurons and HFFs. (A) VZV-infected neuron at 2 days p.i. with an intact double nuclear membrane (NM), normal Golgi apparatus (G), mitochondrion (M), and endoplasmic reticulum (ER). The arrowhead and arrow indicate unenveloped nucleocapsids in the nucleus and enveloped virions on the cell surface, respectively. Magnification, ×6,500. (Inset) Higher magnification of enveloped VZV virions on the surface of the neuron. Bar, 200 nm. (B) VZV-infected HFFs at 2 days p.i. show morphological features of apoptosis, loss of double nuclear membrane, condensed chromatin (Chr), and irregular organelle morphology. An arrow indicates enveloped VZV virions in the cytoplasm. Magnification, ×6,500. (Inset) Higher magnification of enveloped VZV virions in the cytoplasm of the HFF. Bar, 200 nm.

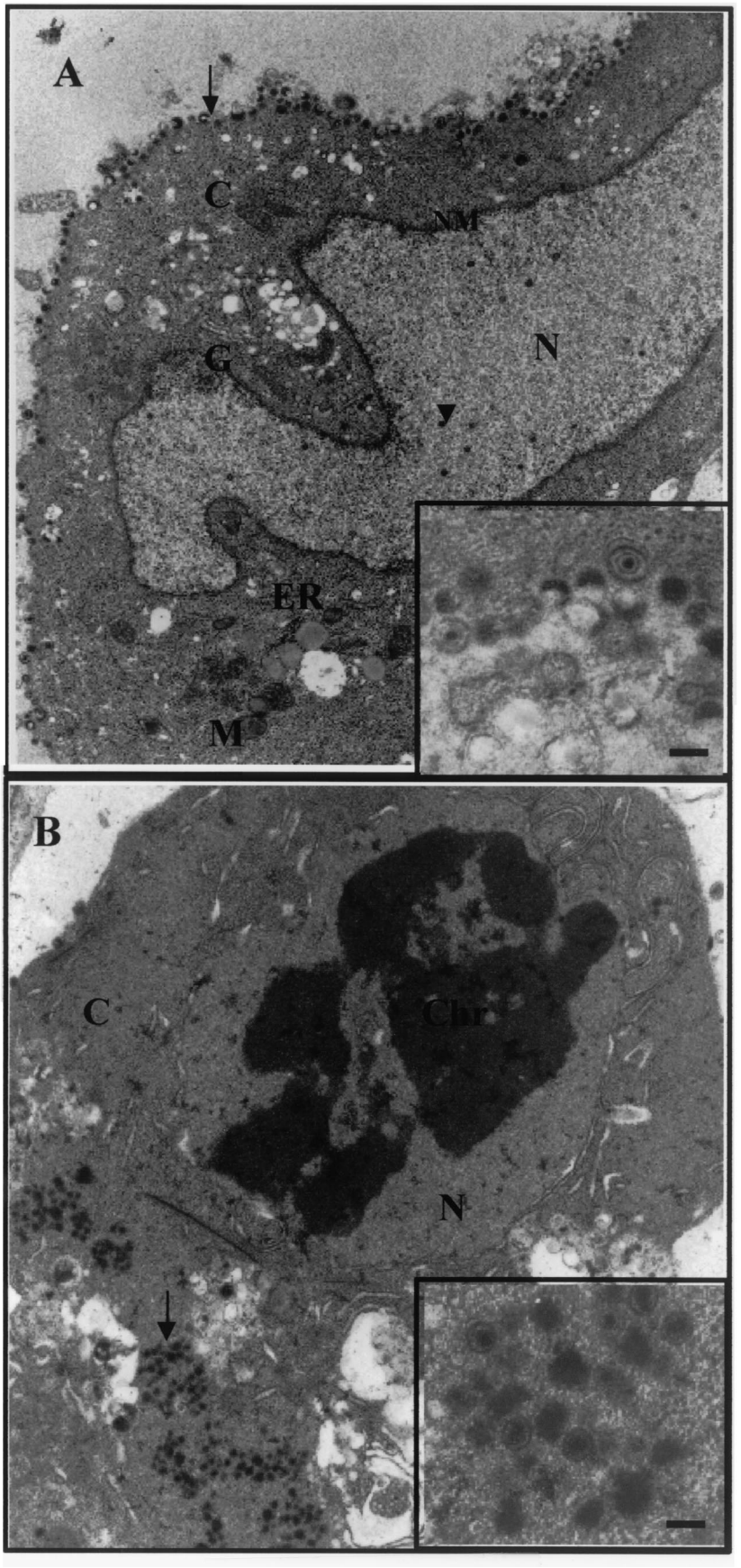
A
C
NM
G
N
ER
M
B
C
Chr
N

latency-associated transcripts expressed by the other alphaherpesvirus family members HSV and BHV have been shown to encode antiapoptotic functions after infection of neurons (1, 11, 55, 71). VZV does not encode an identifiable homologue to either of these latency-associated transcripts. Thus, our additional studies will focus initially on defining the contribution of VZV ORF4, ORF62, ORF63, and ORF66 to the inhibition of apoptosis in neurons.

Unlike infection of primary sensory neurons, we readily detected apoptosis during VZV infection of HFFs. Although VZV gene product(s) associated with the induction of apoptosis needs to be determined, preliminary drug block experiments with phosphonoacetic acid (PAA) suggest that late VZV gene products may be important (data not shown). Studies have shown that HSV-1 induces apoptosis in the presence of cycloheximide, which blocks protein synthesis, suggesting a virion component is necessary for inducing apoptosis (44). In contrast, cycloheximide and PAA treatments of EBV-infected cells demonstrated that EBV early gene products are required for the induction of apoptosis (41). The only herpesvirus gene products identified to encode proapoptotic functions are BHV ORF8, which directly induces apoptosis in rabbit kidney (RK13) cells (53), and the IE gene product US1.5 of HSV-1 (31). Thus, herpesviruses may have evolved a number of distinct proapoptotic mechanisms.

Infection with the low-passage clinical VZV strain Schenke and the high-passage ROka strain both resulted in the induction of apoptosis in HFFs but not in neurons, suggesting that this cell-type-specific apoptotic phenotype is a conserved feature that is VZV strain independent. Although studies with additional clinical isolates of VZV will confirm the conserved nature of this phenotype, studies with clinical and laboratory adapted HSV-1 and HSV-2 strains have sometimes shown a difference in their apoptotic properties. For example, the laboratory-adapted KOS strain but not the clinical HSV-1 isolate CW were shown to induce apoptosis in dissociated rat neurons (A. L. Cunningham, unpublished data). In addition, a laboratory-adapted HSV-2 strain induced apoptosis in Jurkat cells, whereas a clinical isolate of HSV-2 did not (39, 40).

Apoptotic neurons have been detected in central nervous system tissue from individuals with HSV or cytomegalovirus encephalitis (17). Our findings with primary cultured DRG neurons from the peripheral nervous system demonstrate that apoptosis is not a feature of VZV infection of these cells. The impact of VZV on neuronal apoptosis during natural infection will ultimately require an assessment of neurons from immunocompetent patients suffering from active VZV infection at the time of death, and this will be a major focus of our follow-up studies.

The cell-type-specific nature of the apoptotic responses to VZV infection of neurons and HFFs suggests that this virus has evolved different mechanisms that are likely to favor infection of different cell types. Like VZV, other members of the *Alphaherpesvirinae* subfamily, including HSV-1, BHV-1, and pseudorabies virus have also been shown to induce and/or suppress apoptosis in a cell-type-specific manner. HSV-1 can induce apoptosis in many cell types, but it has been reported to be able to suppress apoptosis in neuronal cell lines in vitro and neurons in vivo (55). BHV-1 induces apoptosis in mitogen-stimulated peripheral blood mononuclear cells (32), activated $CD4^+$ T cells (25), epithelial cell lines (21), and dissociated rabbit sensory neurons but not in rabbit trigeminal ganglionic neurons in vivo (19). Furthermore, pseudorabies virus can induce apoptosis in inflammatory cells, such as monocytes/macrophages and lymphocytes; however, it is unable to induce apoptosis in swine trigeminal ganglionic neurons in vivo (2). Thus, among the alphaherpesviruses studied to date, all appear to have evolved mechanisms to suppress apoptosis in neurons, and the present study provides evidence that VZV has done likewise.

In addition to virus-encoded mechanisms, host cell-mediated regulation of apoptosis may also play an important role during VZV infection. In this respect, induction of apoptosis during infection of HFFs may assist the host by limiting the production of progeny virus, whereas inhibition of apoptosis during VZV infection of neurons would promote survival of these nonrenewable, postmitotic cells. Whether a result of a host cell-initiated response to infection or a result of the expression of a specific viral gene product, the antiapoptotic effect observed during infection of neurons is likely to be mutually beneficial to both host and pathogen.

The results obtained in the present study provide evidence that VZV infection results in the regulation of apoptosis in a cell-type-specific manner, a finding that contributes to a more comprehensive understanding of VZV pathogenesis. Both ROka and Schenke strains of VZV were able to induce apoptosis in HFFs and yet were unable to induce apoptosis during infection of sensory neurons. An ability to inhibit apoptosis during infection of neurons may represent a key mechanism involved in the establishment, maintenance, or reactivation phases of VZV latency.

ACKNOWLEDGMENTS

This work was supported by a University of Sydney Medical Foundation grant, a Cecilia Kilkerary Foundation grant, and an NH&MRC project grant 211110. A.A. is the holder of a University of Sydney Rolf Edgar Lake fellowship, and C.H. is the holder of an Australian Postgraduate Award and Westmead Millennium Foundation research scholarship stipend enhancement.

We thank Ann Arvin and Paul Kinchington for VZV gene-specific antibodies and Monica Miranda for assistance with human neuronal cultures.

REFERENCES

1. **Ahmed, M., M. Lock, C. G. Miller, and N. W. Fraser.** 2002. Regions of the herpes simplex virus type 1 latency associated transcript that protect cells from apoptosis in vitro and protect neuronal cells in vivo. J. Virol. **76:**717–729.
2. **Aleman, N., M. I. Quiroga, M. Lopez-Pena, S. Vazquez, F. H. Guerrero, and J. M. Nieto.** 2001. Induction and inhibition of apoptosis by pseudorabies virus in the trigeminal ganglion during acute infection of swine. J. Virol. **75:**469–479.
3. **Aubert, M., A. R. Rice, and J. A. Blaho.** 2001. Accumulation of herpes simplex virus type 1 early and leaky-late proteins correlates with apoptosis prevention in infected human HE-p2 cells. J. Virol. **75:**1013–1030.
4. **Aubert, M., and J. A. Blaho.** 1999. The herpes simplex virus type 1 regulatory protein ICP27 is required for the prevention of apoptosis in infected human cells. J. Virol. **73:**2803–2813.
5. **Aubert, M., J. O'Toole, and J. A. Blaho.** 1999. Induction and prevention of apoptosis in human HEp-2 cells by herpes simplex virus type 1. J. Virol. **73:**10359–10370.
6. **Bartz, S. R., and M. Emerman.** 1999. Human immunodeficiency virus type 1 Tat induces apoptosis and increases sensitivity to apoptotic signals by upregulating FLICE/caspase-8. J. Virol. **73:**1956–1963.
7. **Benedict, C. A., P. S. Norris, and C. F. Ware.** 2002. To kill or be killed: viral evasion of apoptosis. Nat. Immunol. **3:**1013–1018.
8. **Cassady, K. A., M. Gross, and B. Roizman.** 1998. The second site mutation in the herpes simplex virus recombinants lacking the g134.5 genes precludes

shutoff of protein synthesis by blocking the phosphorylation of eIF-2a. J. Virol. **72:**7005–7011.
9. **Cheatham. W. J., W., T. H., T. F. Dolan, and J. C. Dower.** 1956. Varicella: report for fatal two fatal cases with necropsy, virus isolation and serologic studies. Am. J. Pathol. **32:**1015–1035.
10. **Chou, J., and B. Roizman.** 1992. The gamma 1(34.5) gene of herpes simplex virus 1 precludes neuroblastoma cells from triggering total shutoff of protein synthesis characteristic of programed cell death in neuronal cells. Proc. Natl. Acad. Sci. USA **89:**3266–3270.
11. **Ciacci-Zanella, J., J. Stone, G. Henderson, and C. Jones.** 1999. The latency-related gene of bovine herpesvirus 1 inhibits programmed cell death. J. Virol. **73:**9734–9740.
12. **Cohen, J. I., and S. E. Straus.** 2001. Varicella-zoster virus and its replication, p. 2707–2730. *In* D. M. Knipe and P. M. Howley (ed.), Fields virology, 4th ed. Lippincott/The Williams & Wilkins Co., Philadelphia, Pa.
13. **Cohen, J. I., and K. E. Seidel.** 1993. Generation of varicella-zoster virus (VZV) and viral mutants from cosmid DNAs: VZV thymidylate synthetase is not essential for replication in vitro. Proc. Natl. Acad. Sci. USA **90:**7376–7380.
14. **Cohrs, R. J., M. Barbour, and D. H. Gilden.** 1996. Varicella-zoster virus (VZV) transcription during latency in human ganglia: detection of transcripts mapping to genes 21, 29, 62, and 63 in a cDNA library enriched for VZV RNA. J. Virol. **70:**2789–2796.
15. **Conti, L., P. Matarrese, B. Varano, M. C. Gauzzi, A. Sato, W. Malorni, F. Belardelli, and S. Gessani.** 2000. Dual role of the HIV-1 vpr protein in the modulation of the apoptotic response of T cells. J. Immunol. **165:**3293–3300.
16. **Croen, K. D., J. M. Ostrove, L. J. Dragovic, and S. E. Straus.** 1988. Patterns of gene expression and sites of latency in human nerve ganglia are different for varicella-zoster and herpes simplex viruses. Proc. Natl. Acad. Sci. USA **85:**9773–9777.
17. **DeBiasi, R. L., B. K. Kleinschmidt-DeMasters, S. Richardson-Burns, and K. L. Tyler.** 2002. Central nervous system apoptosis in human herpes simplex virus and cytomegalovirus encephalitis. J. Infect. Dis. **186:**1547–1557.
18. **Debrus, S., C. Sadzot-Delvaux, A. F. Nikkels, J. Piette, and B. Rentier.** 1995. Varicella-zoster virus gene 63 encodes an immediate-early protein that is abundantly expressed during latency. J. Virol. **69:**3240–3245.
19. **Delhon, G. A., M. J. Gonzalez, and P. R. Murcia.** 2002. Susceptibility of sensory neurons to apoptosis following infection by bovine herpesvirus type 1. J. Gen. Virol. **83:**2257–2267.
20. **Denny-Brown, D., R. Adam, and P. Fitzgerald.** 1944. Pathologic features of herpes zoster. Am. Med. Assoc. Arch. Dermatol. **75:**193–196.
21. **Devireddy, L. R., and C. J. Jones.** 1999. Activation of caspases and p53 by bovine herpesvirus 1 infection results in programmed cell death and efficient virus release. J. Virol. **73:**3778–3788.
22. **Djerbi, M., V. Screpanti, A. I. Catrina, B. Bogen, P. Biberfeld, and A. Grandien.** 1999. The inhibitor of death receptor signaling, FLICE-inhibitory protein defines a new class of tumor progression factors. J. Exp. Med. **190:**1025–1032.
23. **Duncan, R., A. Esmaili, L. M. Law, S. Bertholet, C. Hough, T. C. Hobamn, and H. L. Nakhasi.** 2000. Rubella virus capsid protein induces apoptosis in transfected RK13 cells. Virology **275:**20–29.
24. **Elliott. K. J.** 2000. Managment of postherpetic pain, p. 412–427. *In* A. A. Gershon (ed.), Varicella zoster virus: virology and clinical management. Cambridge University Press, Cambridge, United Kingdom.
25. **Eskra, L., and G. A. Splitter.** 1997. Bovine herpesvirus-1 infects activated $CD4^+$ lymphocytes. J. Gen. Virol. **78:**2159–2166.
26. **Fadok, V. A., D. R. Voelker, P. A. Campbell, J. J. Cohen, D. L. Bratton, and P. M. Henson.** 1992. Exposure of phosphatidylserine on the surface of apoptotic lymphocytes triggers specific recognition and removal by macrophages. J. Immunol. **148:**2207–2216.
27. **Gavrieli, Y., Y. Sherman, and S. A. Ben-Sasson.** 1992. Identification of programmed cell death in situ via specific labeling of nuclear DNA fragmentation. J. Cell Biol. **119:**493–501.
28. **Gilden, D. H., B. K. Kleinschmidt-DeMasters, J. J. LaGuardia, R. Mahalingam, and R. J. Cohrs.** 2000. Neurologic complications of the reactivation of varicella-zoster virus. N. Engl. J. Med. **342:**635–645. (Erratum, **342:** 1063.)
29. **Gilden, D. H., A. Vafai, Y. Shtram, Y. Becker, M. Devlin, and M. Wellsih.** 1983. Varicella-zoster virus DNA in human sensory ganglia. Nature **306:**378–480.
30. **Griebel, P., H. B. Ohmann, J. P. Lawman, and L. A. Babiuk.** 1990. The interaction of between bovine herpesvirus type 1 and activated bovine T lymphocytes. J. Gen. Virol. **71:**369–377.
31. **Hagglund, R., J. Munger, A. P. Poon, and B. Roizman.** 2002. U(S)3 protein kinase of herpes simplex virus 1 blocks caspase 3 activation induced by the products of U(S)1.5 and U(L)143 genes and modulates expression of transduced U(S)1.5 open reading frame in a cell type-specific manner. J. Virol. **76:**743–754.
32. **Hanon, E., A. Vanderplasschen, S. Lyaku, G. Keil, M. Denis, and P. P. Pastoret.** 1996. Inactivated bovine herpesvirus 1 induces apoptotic cell death of mitogen-stimulated bovine peripheral blood mononuclear cells. J. Virol. **70:**4116–4120.
33. **Hata, S., A. H. Koyama, H. Shiota, A. Adachi, F. Goshima, and Y. Nishiyama.** 1999. Antiapoptotic activity of herpes simplex virus type 2: the role of US3 protein kinase gene. Microbes Infect. **1:**601–607.
34. **Hay, S., and G. Kannourakis.** 2002. A time to kill: viral manipulation of the cell death program. J. Gen. Virol. **83:**1547–1564.
35. **Head, H., and A. W. Campbell.** 1900. The pathology of herpes zoster and its bearing on sensory localization. Brain **23:**353–523.
36. **Hope-Simpson, R. E.** 1975. Post-herpetic neuralgia. J. R. Coll. Gen. Pract. **25:**571–575.
37. **Hyman, R. W., J. R. Ecker, and R. B. Tenser.** 1983. Varicella-zoster virus RNA in human trigeminal ganglia. Lancet **ii:**814–816.
38. **Ito, M., M. Watanabe, H. Kamiya, and M. Sakurai.** 1997. Herpes simplex virus type 1 induces apoptosis in peripheral blood T lymphocytes. J. Infect. Dis. **175:**1220–1224.
39. **Jerome, K. R., R. Fox, Z. Chen, P. Sarkar, and L. Corey.** 2001. Inhibition of apoptosis by primary isolates of herpes simplex virus. Arch. Virol. **146:**2219–2225.
40. **Jerome, K. R., R. Fox, Z. Chen, A. E. Sears, H. Lee, and L. Corey.** 1999. Herpes simplex virus inhibits apoptosis through the action of two genes, Us5 and Us3. J. Virol. **73:**8950–8957.
41. **Kawanishi, M.** 1993. Epstein-Barr virus induces fragmentation of chromosomal DNA during lytic infection. J. Virol. **67:**7654–7658.
42. **Kawanishi, M.** 1997. Expression of Epstein-Barr virus latent membrane protein 1 protects Jurkat T cells from apoptosis induced by serum deprivation. Virology **228:**244–250.
43. **Kinchington, P. R., and J. I. Cohen.** 2000. Varicella zoster virus proteins, p. 74–104. *In* A. A. Gershon (ed.), Varicella zoster virus: virology and clinical management. Cambridge University Press, Cambridge, United Kingdom.
44. **Koyama, A. H., and A. Adachi.** 1997. Induction of apoptosis by herpes simplex virus type 1. J. Gen. Virol. **78:**2909–2912.
45. **Leopardi, R., and B. Roizman.** 1996. The herpes simplex virus major regulatory protein ICP4 blocks apoptosis induced by the virus or by hyperthermia. Proc. Natl. Acad. Sci. USA **93:**9583–9587.
46. **Leopardi, R., C. Van Sant, and B. Roizman.** 1997. The herpes simplex virus 1 protein kinase US3 is required for protection from apoptosis induced by the virus. Proc. Natl. Acad. Sci. USA **94:**7891–7896.
47. **Li, C. J., D. J. Friedman, C. Wang, V. Metelev, and A. B. Pardee.** 1995. Induction of apoptosis in uninfected lymphocytes by HIV-1 Tat protein. Science **268:**429–431.
48. **Low, H., M. Harries, H. Ye, M. Q. Du, C. Bosshoff, and M. Collins.** 2001. Internal ribosome entry site regulates translation of Kaposi's sarcoma-associated herpesvirus FLICE inhibitory protein. J. Virol. **75:**2938–2945.
49. **Lungu, O., C. A. Panagiotidis, P. W. Annunziato, A. A. Gershon, and S. J. Silverstein.** 1998. Aberrant intracellular localization of varicella-zoster virus regulatory proteins during latency. Proc. Natl. Acad. Sci. USA **95:**7080–7085.
50. **Marshall, W. L., C. Yim, E. Gustafson, T. Graf, D. R. Sage, K. Hanify, L. Williams, J. Fingeroth, and R. W. Finberg.** 1999. Epstein-Barr virus encodes a novel homolog of the bcl-2 oncogene that inhibits apoptosis and associates with Bax and Bak. J. Virol. **73:**5181–5185.
51. **Miranda-Saksena, M., P. Armati, R. A. Boadle, D. J. Holland, and A. L. Cunningham.** 2000. Anterograde transport of herpes simplex virus type 1 in cultured, dissociated human and rat dorsal root ganglion neurons. J. Virol. **74:**1827–1839.
52. **Munger, J., A. V. Chee, and B. Roizman.** 2001. The U(S)3 protein kinase blocks apoptosis induced by the d120 mutant of herpes simplex virus 1 at a premitochondrial stage. J. Virol. **75:**5491–5497.
53. **Nakamichi, K., Y. Matsumoto, Y. Tohya, and H. Otsuka.** 2002. Induction of apoptosis in rabbit kidney cell under high-level expression of bovine herpesvirus 1 U(s) ORF8 product. Intervirology **45:**85–93.
54. **O'Brien, V.** 1998. Viruses and apoptosis. J. Gen. Virol. **79:**1833–1845.
55. **Perng, G. C., C. Jones, J. Ciacci-Zanella, M. Stone, G. Henderson, A. Yukht, S. M. Slanina, F. M. Hofman, H. Ghiasi, A. B. Nesburn, and S. L. Wechsler.** 2000. Virus-induced neuronal apoptosis blocked by the herpes simplex virus latency-associated transcript. Science **287:**1500–1503.
56. **Posavad, C. M., J. J. Newton, and K. L. Rosenthal.** 1994. Infection and inhibition of human cytotoxic T lymphocytes by herpes simplex virus. J. Virol. **68:**4072–4074.
57. **Pugachev, K. V., and T. K. Frey.** 1998. Rubella virus induces apoptosis in cultured cells. Virology **250:**359–370.
58. **Raftery, M. J., C. K. Behrens, A. Muller, P. H. Krammer, H. Walczak, and G. Schonrich.** 1999. Herpes simplex virus type 1 infection of activated cytotoxic T cells: induction of fratricide as a mechanism of viral immune evasion. J. Experi. Med. **190:**1103–1114.
59. **Randazzo, B. P., R. Tal-Singer, J. M. Zabolotny, S. Kesari, and N. W. Fraser.** 1997. Herpes simplex virus 1716, an ICP 34.5 null mutant, is unable to replicate in CV-1 cells due to a translational block that can be overcome by coinfection with SV40. J. Gen. Virol. **78:**3333–3339.
60. **Sadzot-Delvaux, C., P. Thonard, S. Schoonbroodt, J. Piette, and B. Rentier.** 1995. Varicella-zoster virus induces apoptosis in cell culture. J. Gen. Virol. **76:**2875–2879.
61. **Shen, Y., and T. E. Shenk.** 1995. Viruses and apoptosis. Curr. Opin. Genet. Devel. **5:**105–111.

62. **Silverstein, S., and S. Straus.** 2000. Pathogenesis of latency and reactivation, p. 123–141. *In* A. A. Gershon (ed.), Varicella zoster virus. Virology and clinical management. Cambridge University Press, Cambridge, United Kingdom.
63. **Skaletskaya, A., L. M. Bartle, T. Chittenden, A. L. McCormick, E. S. Mocarski, and V. S. Goldmacher.** 2001. A cytomegalovirus-encoded inhibitor of apoptosis that suppresses caspase-8 activation. Proc. Natl. Acad. Sci. USA **98:**7829–7834.
64. **Stevenson, D., K. L. Colman, and A. J. Davison.** 1994. Characterization of the putative protein kinases specified by varicella-zoster virus genes 47 and 66. J. Gen. Virol. **75:**317–326.
65. **Sturzl, M., C. Hohenadl, C. Zietz, E. Castanos-Velez, A. Wunderlich, G. Ascherl, P. Biberfeld, P. Monini, P. J. Browning, and B. Ensoli.** 1999. Expression of K13/v-FLIP gene of human herpesvirus 8 and apoptosis in Kaposi's sarcoma spindle cells. J. Natl. Cancer Inst. **91:**1725–1733.
66. **Su, F., and R. J. Schneider.** 1997. Hepatitis B virus HBx protein sensitizes cells to apoptotic killing by tumor necrosis factor alpha. Proc. Natl. Acad. Sci. USA **94:**8744–8749.
67. **Su, F., C. N. Theodosis, and R. J. Schneider.** 2001. Role of NF-κB and myc proteins in apoptosis induced by hepatitis B virus HBx protein. J. Virol. **75:**215–225.
68. **Takashima, S., and L. E. Bechler.** 1979. Neuropathology of fatal varicella. Arch. Pathol. Lab. Med. **103:**209–213.
69. **Taylor-Robinson, D., and A. E. Caunt.** 1972. Varicella virus. Springer-Verlag, Berlin, Germany.
70. **Teodoro, J. G., and P. E. Branton.** 1997. Regulation of apoptosis by viral gene products. J. Virol. **71:**1739–1746.
71. **Thomson, R. L., and N. M. Sawtell.** 2001. Herpes simplex virus type 1 latency associated transcript gene promotes neuronal survival. J. Virol. **75:**6660–6675.
72. **Trump, B. F., and I. K. Berezesky.** 1998. The reaction of cells to lethal injury: oncosis and necrosis: the role of calcium, p. 57–96. *In* R. A. Lockshim, Z. Zakeri, and J. L. Tilly (ed.), When cells die: a comprehensive evaluation of apoptosis and programmed cell death. Wiley-Liss, New York, N.Y.
73. **Vaux, D. L., and A. Strasser.** 1996. The molecular biology of apoptosis. Proc. Natl. Acad. Sci. USA **93:**2239–2244.
74. **Watson, C. P. N., and J. H. Deck.** 1993. The neuropathology of herpes zoster with particular reference to postherpetic neuralgia and its pathogenesis, p. 139–157. *In* C. P. N. Watson (ed.), Herpes zoster and postherpetic neuralgia, vol. 8. Pain research and clinical management. Elsevier, New York, N.Y.
75. **Watson, C. P. N., J. H. Deck, C. Morshead, et al.** 1991. Post-herpetic neuralgia: further post-mortem studies of cases with or without pain. Pain **44:**105–117.
76. **Weller, T. H.** 1953. Serial propagation in vitro of agents producing inclusion bodies derived from varicella and herpes zoster. Proc. Soc. Exp. Biol. **83:** 340–346.
77. **Weller, T. H.** 1983. Varicella and herpes zoster: changing concepts of the natural history: control and importance of a not-so-benign virus. N. Engl. J. Med. **309:**1362.
78. **White, E.** 1996. Life, death, and the pursuit of apoptosis. Genes Dev. **10:**1–15.
79. **Winkler, M. T., A. Doster, and C. Jones.** 1999. Bovine herpesvirus 1 can infect $CD4^+$ T lymphocytes and induce programmed cell death during acute infection of cattle. J. Virol. **73:**8657–8668.
80. **Young, L. S., C. W. Dawson, and A. G. Eliopoulos.** 1999. Epstein-Barr virus and apoptosis: viral mimicry of cellular pathways. Biochem. Soc. Trans. **27:**807–812.
81. **Zhou, G., and B. Roizman.** 2001. The domains of glycoprotein D required to block apoptosis depend on whether glycoprotein D is present in the virions carrying herpes simplex virus 1 genome lacking the gene encoding the glycoprotein. J. Virol. **75:**6166–6172.
82. **Zhu, H., Y. Shen, and T. Shenk.** 1995. Human cytomegalovirus IE1 and IE2 proteins block apoptosis. J. Virol. **69:**7960–7970.